

Ecclesiastical heritage, territory and society: Knowledge tools and historical-critical debate

*Original*

Ecclesiastical heritage, territory and society: Knowledge tools and historical-critical debate / Longhi, A.. - In: IN BO. - ISSN 2036-1602. - ELETTRONICO. - 12:6(2021), pp. 46-59. [10.6092/issn.2036-1602/12352]

*Availability:*

This version is available at: 11583/2938276 since: 2021-11-16T22:19:43Z

*Publisher:*

University of Bologna

*Published*

DOI:10.6092/issn.2036-1602/12352

*Terms of use:*

This article is made available under terms and conditions as specified in the corresponding bibliographic description in the repository

*Publisher copyright*

(Article begins on next page)





the four-wave-mixing part is considered negligible [14], it is solely due to the cross phase modulation (XPM) of a 10G channel on a 100G channel. As for the self channel penalty, i.e. the self-phase modulation (SPM) of the coherent channel on a DM OLS, it is out of the scope of this study, since it does not depend on the IMDD channels and could also be compensated for with appropriate equalization techniques at the DSP receiver.

The 10G-to-100G XPM interaction in DM-OLS manifests as a multiplicative non-linear phase noise (NLPN) and as an additive noise-like contribution. The NLPN component derives from the pure phase modulation of the 100G channel by the 10G probe. However, it can be completely recovered by carrier phase estimation (CPE) algorithms [14]. The additive noise-like contribution instead originates mainly by the interplay between the XPM effect and the polarization effects as birefringence and polarization mode dispersion (PMD) [15], [16]. This contribution is peculiar of the interaction between 100G and 10G channels, since the latter are *polarized* signals, opposite to the *depolarized* 100G channels. Following our previous investigations in [14], [16], in the following sections we refine our semi-analytical method for the estimation of the joint XPM-Polarization noise contribution.

While in this first section we have framed the context and described briefly the major issues, in section II we will first introduce the concepts behind the network and OLS abstraction as weighted graph. This abstraction is then employed by the SDN and OLS controllers blocks to perform path computation and distinguish between the single, independent noise sources setting the GSNR. We then proceed by presenting the semi-analytical model developed for the estimation of the joint XPM-polarization noise, which is both *spectrally* and *spatially* disaggregated. This simple-yet-effective model, serving as a QoT-E software module, is then validated by comparing its result with Split-Step Fourier method (SSFM) based simulations in section III, showing that it provides QoT predictions which are always conservative. Finally, in section IV, conclusions are drawn and future improvements are proposed.

## II. MODELING THE PHYSICAL LAYER

### A. The network abstraction

In order to perform optical path discovery and feasibility the SDN controller must elaborate an abstraction of the optical network with respect to the chosen QoT metric. This is done by representing the optical network as a weighted graph, as depicted in Fig.2. The nodes of the graph coincide with the add-drop sites, allowing to route transparently single lightpath through the network, while the edges are the OLSs. Edges are weighted by the QoT merit figure. As previously mentioned, the GSNR can be taken as the unique merit for QoT [4]. Hence, each edge between two nodes is labelled with the GSNR degradation experienced by the considered channel throughout the OLS, given by:

$$\text{GSNR} = \frac{P_{ch}}{P_{N,TOT}} \quad (1)$$

where  $P_{ch}$  is the 100G channel launched optical power and  $P_{N,TOT}$  is the sum of all the noise sources. The validity of GSNR as general QoT metric holds as long as the lightpath can be modeled as an AWGN channel, that is, if all the impairments in  $P_{N,TOT}$  can be modelled as gaussian distributed noise sources summing up independently. This OLS abstraction is used to calculate the path QoT, as represented in Fig.2, where fiber introduces only a loss and the noise sources are lumped and added after an ideal gain. By considering the inverse of the GSNR, is possible to write additively the single noise contributions as in Eq.2:

$$\frac{1}{\text{GSNR}} = \frac{1}{\text{OSNR}} + \frac{1}{\text{SNR}_{\text{NLI}}} + \frac{1}{\text{SNR}_{\text{SPM}}} + \frac{1}{\text{SNR}_{\text{NL-10G}}} \quad (2)$$

The GSNR takes into account all the significant impairments. However, in Eq.2 and throughout the paper we can assume that these are only the ASE noise coming from optical amplifiers and the non-linear noise sources without any loss of generality.

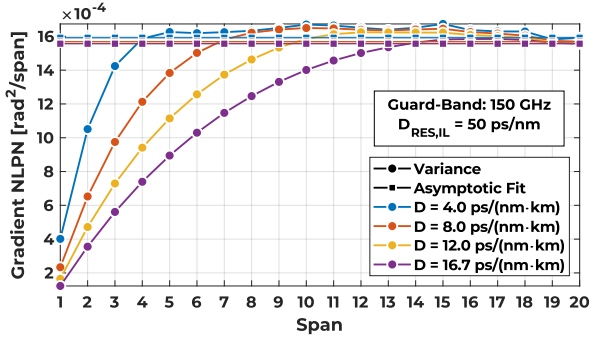
In Eq.2, OSNR is determined by the amplified spontaneous emission (ASE) noise of the optical amplifiers.  $\text{SNR}_{\text{NLI}}$  includes the non-linear noise generated by the propagation of the 100G channels on the uncompensated network, which is known to be modelled as additive and gaussian. [5], [9].

$\text{SNR}_{\text{SPM}}$  instead is the noise contribution due to the single channel propagation over the DM system and can be regarded as an NLI-like noise provided that the DM link has not full dispersion compensation ( $D_{\text{RES,IL}} = 0$  ps/nm). However, this configuration is absolutely detrimental for both coherent and IMDD signals and avoided in practical system configurations. In any case, the study of this term is out of the scope of the paper.

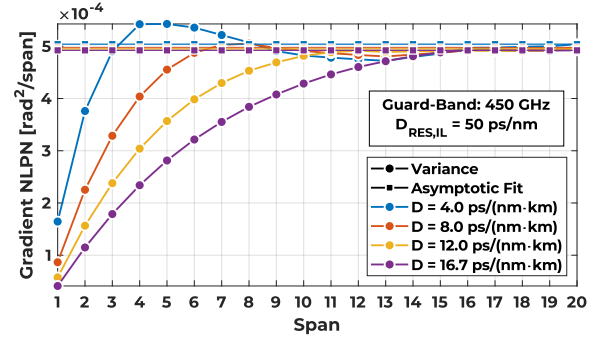
Finally, the  $\text{SNR}_{\text{NL-10G}}$  term encompasses the non-linear noise due to the XPM of 10G channels populating the DM OLS on the 100G channels and its estimation is the goal of the tool presented in this work. As already mentioned, the XPM manifests as a multiplicative NLPN component and an additive noise component due to the polarization coupling effects [16]. However, practical DSP-based receivers are able to completely compensate the XPM phase noise [14] thanks to the Carrier Phase Estimator (CPE) stage, so that the whole XPM effect is included in the  $\text{SNR}_{\text{NL-10G}}$  within the GSNR.

### B. Modeling the mixed 10G-100G XPM

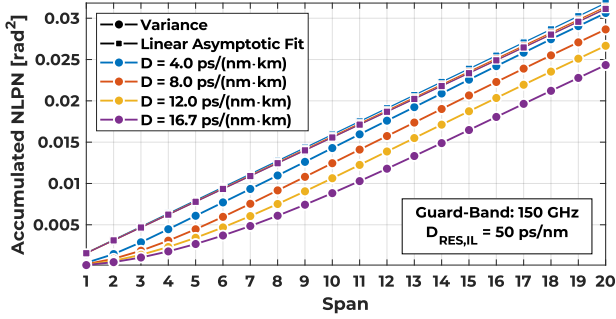
The  $\text{SNR}_{\text{NL-10G}}$  is due to the additive noise contribution arising from the XPM and birefringence interaction. Its entity thus depends on the relative polarization angle  $\Omega$  between the polarized 10G channels and the 100G channel independently-modulated polarization components (namely, the X and Y components). Also, it depends on the evolution of the polarization rotations induced by the birefringence due to its stochastic nature, which randomly couple the two 100G polarization states. A rigorous mathematical modelling would require a complex stochastic solution of the Coupled Non-Linear Schrodinger equation (CNLSE), which is out of the scope of this study. Here instead the goal is to provide a simple QoT-E tool suitable to plan and provision lightpaths



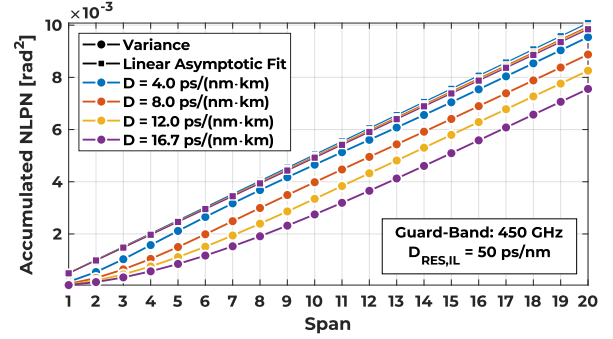
(a)



(a)



(b)



(b)

Fig. 3: NLPN gradient (a) and accumulation (b) for pump and probe spaced 150 GHz at  $D_{RES,IL} = 50$  ps/nm

Fig. 5: NLPN gradient (a) and accumulation (b) for pump and probe spaced 450 GHz at  $D_{RES,IL} = 50$  ps/nm

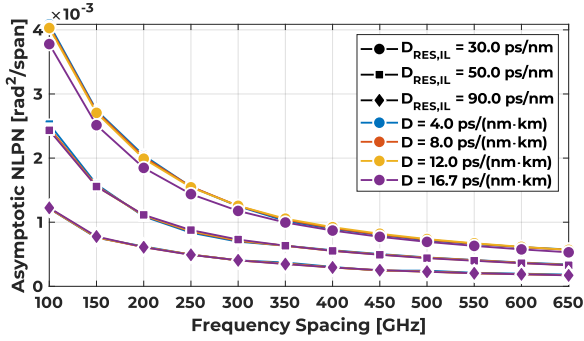


Fig. 4: Pump and probe asymptotic NLPN per span vs guard-band, dispersion coefficient and inline residual dispersion

along both the 10G and 100G network. For this purpose, we add two requirements on the model:

- *Spectral Disaggregation*: the  $SNR_{NL-10G}$  degradation on a 100G channel (the *probe*) caused by the effect of  $N_p$  10G channels (the *pumps*) is given by the inverse sum of the  $SNR_{NL-10G}$  contribution of each pump, as in Eq.3

$$\frac{1}{SNR_{NL-10G}} = \sum_{k=1}^{N_p} \frac{1}{SNR_{NL-10G,k}} \quad (3)$$

where  $SNR_{NL-10G,k}$  is the SNR degradation determined by the noise of the  $k$ -th 10G pump.

- *Spatial Disaggregation*: the  $SNR_{NL-10G,k,n}$  of the  $k$ -th 10G pump introduced by the  $n$ -th fiber span does not depend on the previous spans traveled but only on the span itself, so that, after  $N_s$  fiber spans Eq.4 holds:

$$\frac{1}{SNR_{NL-10G,k}} = \sum_{n=1}^{N_s} \frac{1}{SNR_{NL-10G,k,n}} \quad (4)$$

To fulfill these requirements, we propose a simpler approach assuming that the stochastic birefringence-induced polarization rotations transform the NLPN written by the 10G on the 100G X and Y components in an additive noise crosstalk due to the polarization coupling. In order to develop this abstraction we started to observe the XPM phenomenon by propagating a single polarization mode per 100G/10G channel in Split-Step Fourier (SSFM) simulations in the worst-case of polarization alignment. In [14] we have shown that, in this case, thus without any polarization rotations, the 10G-to-100G XPM is essentially an NLPN writing. We have also proved that the NLPN can be spectrally disaggregated as it sums up in variance for each 10G pump turned on [14]. The amount of worst-case, polarization-aligned NLPN is obtained by single polarization SSFM simulations on the 20x fiber span setup of Fig.2(b) by turning off the CPE stage. The NLPN is computed as the variance of the optical phase extracted as the ratio between the received and the transmitted 100G signals, under the XPM generated by a single 10G pump placed at increasing frequency spacing in the 50 GHz grid. We have

also studied the spatial accumulation of the NLPN. Fig.3-5(a) plots a sample amount of NLPN introduced by each fiber span. They shows that, after a transient depending on the fiber chromatic dispersion coefficient, the NLPN gradient converges to the same asymptotic value. Fig.3-5(b) also report the accumulated NLPN, also the linear fit obtained using the asymptotic amount of NLPN per span, showing that, in any case, after a transient, the growing is substantially linear. This enables spatial disaggregation: the amount of accumulated NLPN can be conservatively approximated span by span, without apriori knowledge of the whole OLS. These peculiarities can be also seen by plotting the asymptotic NLPN behavior vs the frequency distance between the 100G probe and a 10G pump, as in Fig.4. The NLPN intensity does not depend on the absolute value of the fiber span chromatic dispersion but only on the amount of residual inline dispersion  $D_{RES,IL}$ .

Following the derivation in [16], we then use the polarization-aligned asymptotic NLPN variance to calculate the crosstalk noise due to the insertion of the polarization rotations, so that, the  $SNR_{NL,10G}$  degradation introduced by the k-th 10G pump by the n-th fiber span of the OLS is given by:

$$SNR_{NL,10G,k,n} = \frac{1}{\sin^2 2\theta_n E[|\sin \Delta\phi_{e,k}(t)|^2]} \quad (5)$$

As in [14], [16],  $\Delta\phi_{e,k}(t)$  is a differential NLPN term depending on the initial relative polarization angle  $\Omega$  between the k-th 10G pump and 100G channel.

When the 10G pump is aligned with the X or Y polarizations of the 100G probe, the NLPN differential term is maximum, otherwise, the initial polarization-aligned NLPN is split between the two X and Y 100G polarization components accordingly to simple sine/cosine relationships. The angle  $\theta_n$  is an equivalent polarization rotation due to birefringence relative to the n-th span which is set to the worst case value of  $45^\circ$  to stay conservative. Using Eq.5 together with Eq.3,4 delivers a very simple and fast estimation of the  $SNR_{NL,10G}$  degradation of a single fiber span, which sums up with the inverse SNR relationship over a complete multispan OLS and  $N_p$  10G channels.

### III. QOT-ESTIMATOR TOOL VALIDATION

In this section we compare the  $SNR_{NL,10G}$  estimation of Eq.3-5 with the results obtained by SSFM Monte-Carlo simulation campaign on the setup of Fig.2. We have considered a 20x 50 km long fiber spans with loss  $\alpha = 0.18$  dB/km, non-linear coefficient  $\gamma = 1.27$  (W · km)<sup>-1</sup> and chromatic dispersion  $D = 4.0$  ps/(nm · km), and 16.7 ps/(nm · km). 100G probe channel is PM-QPSK modulated with  $R_s = 32$  GBaud and its power is always kept sufficiently low to avoid SPM. Optical amplifiers are also noiseless, so that the GSNR estimated by our DSP implementation corresponds to the  $SNR_{NL,10G}$  alone in Eq.2. DSP implements an LMS equalizer with 42 taps followed by a Viterbi-Viterbi [17] CPE stage recovering any residual NLPN.

Although other maps have been tested, here we focused on two dispersion map, one leaves nearly  $D_{RES,IL} = 50$  ps/nm of inline residual dispersion as this is the most common value

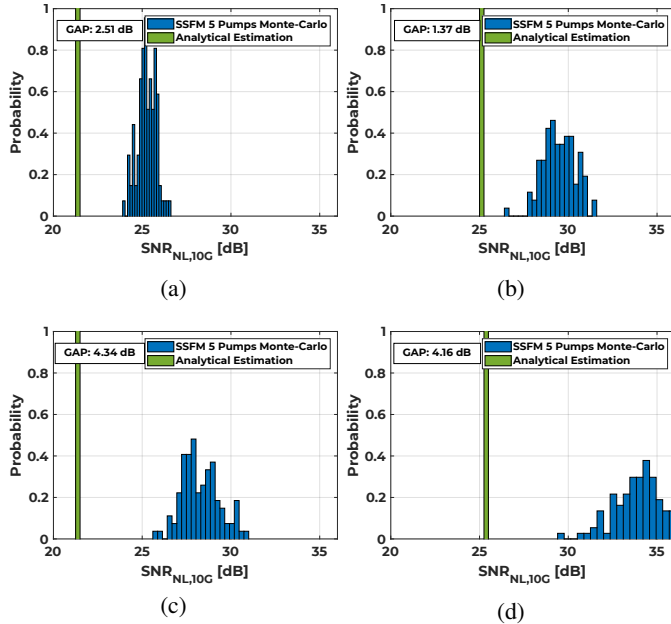


Fig. 6: Model vs SSFM 5 pumps Monte-Carlo simulations at  $D_{RES,IL} = 50$  ps/nm:  $D = 4$  (upper row), 16.7 ps/(nm · km) (lower row). Frequency spacing: 150 GHz (left), 450 GHz (right)

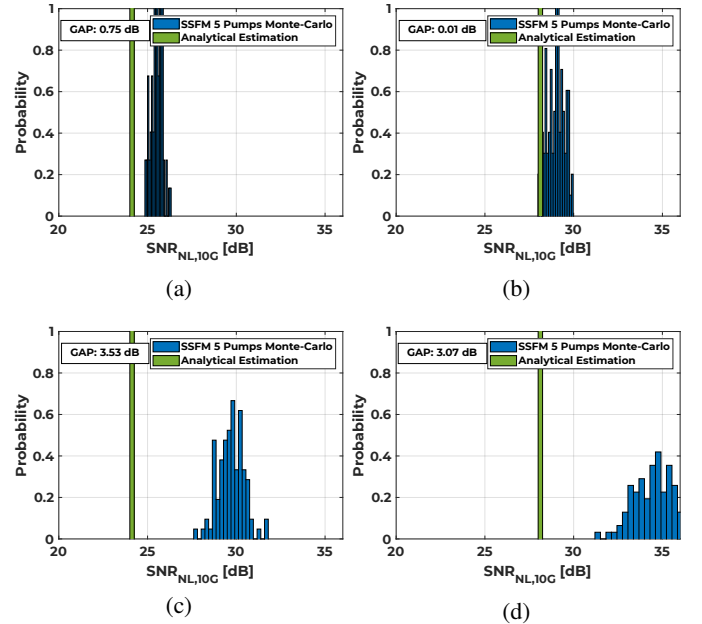


Fig. 7: Model vs SSFM 5 pumps Monte-Carlo simulations at  $D_{RES,IL} = 90$  ps/nm:  $D = 4$  (upper row), 16.7 ps/(nm · km) (lower row). Frequency spacing: 150 GHz (left), 450 GHz (right)

in deployed systems, the other has  $D_{RES,IL} = 90$  ps/nm to take into account realistic deviation from the nominal residual because of DCU granularity or further dispersive elements such as filters.

The model has been tested in a multi-pump and single probe configuration with 5 x 10G pumps. The  $SNR_{NL-10G}$  estimation has been obtained for each pump using Eq.5 and added up with Eq.3,4. This has been done for the two dispersion values considered and pump-probe frequency spacing of 150 and 450 GHz. Here, we have set  $\Omega = 22.5^\circ$  as the 10G/100G polarization angle delivering the more accurate estimations with respect to Monte-Carlo simulations. The results are reported in Fig.6 and Fig.7 for  $D_{RES,IL} = 50, 90$  ps/nm, respectively, together with the gap between the modeling tool result and the simulated PDF worst-case  $SNR_{NL-10G}$ . The estimation scales correctly with the guard-band between the 100G probe and the 10G comb and the inline residual dispersion, although the gap increases at larger guard-bands and dispersion coefficients. However, the model is always conservative, thus letting operation of the light path always in the safe side and avoiding out of service. Note that the independence of the results on dispersion coefficient is a direct consequence of the same independence of asymptotic NLPN per span of Fig.4. In fact, using the asymptotic value, on one side ignores the different transient dispersion coefficient dependent of Fig.3,5(a), on the other side, however, enables spatial disaggregation and thus an fast and simple QoT estimation and path computation. As for the estimation accuracy with respect to SSFM simulations worst case, we get a maximum gap of 4.34 dB and 3.53 dB for  $D_{RES,IL} = 50, 90$  ps/nm, respectively. It should be noted that, although the accuracy could be improved in these cases, this margin is not the overall GSNR margin but only with respect to the inter-channel part of the non-linear interferences on the 10G-DM OLS, thus having a less important weight when considering all the noise contributions in the GSNR as in Eq.2.

#### IV. CONCLUSIONS

In this work we have discussed and proposed solution to the problem of the mixed propagation of coherent and IMDD channels on dispersion-compensated optical networks. This is a useful opportunity in the market to save on CAPEX for the upgrade on 10G networks to coherent transmission technology. Also being able to do this will enable further network routing flexibility, enabling routing of 100G channels through sections of metro DM networks already loaded with 10G channels. In this work we have proposed a QoT-E tailored to be implemented in the network control plane which is able to quickly (seconds timescale) and efficiently estimate the GSNR penalty due to the inter-channel non-linear interaction between the 100G channels and 10G channels. The tool has shown to provide always conservative QoT estimation, with respect to the worst-case GSNR obtained by accurate SSFM Monte-Carlo simulation campaigns. In addition, the model is spectrally and spatially disaggregated: this allows the network control plan to perform lightpath provisioning in a traffic-

agnostic fashion, i.e. without knowing the propagation history of the coherent channels. Although the Further investigation will be focused on improving accuracy and assessing their impact on the network performance metrics.

#### ACKNOWLEDGMENT

This work has been supported by SM-Optics within a research project

#### REFERENCES

- [1] A. Ferrari, M. Filer, K. Balasubramanian, Y. Yin, E. Le Rouzic, J. Kundrat, G. Grammel, G. Galimberti, and V. Curri, "Gnpy: an open source application for physical layer aware open optical networks," *IEEE/OSA Journal of Optical Communications and Networking*, vol. 12, no. 6, pp. C31–C40, 2020.
- [2] A. C. et al., "Odn: Open disaggregated transport network. discovery and control of a disaggregated optical network through open source software and open apis," in *OFC 2019*, pp. 1–3, 2019.
- [3] R. Casellas, R. Martínez, R. Vilalta, and R. Muñoz, "Abstraction and control of multi-domain disaggregated optical networks with openroadm device models," *Journal of Lightwave Technology*, vol. 38, no. 9, pp. 2606–2615, 2020.
- [4] M. Filer, M. Cantono, A. Ferrari, G. Grammel, G. Galimberti, and V. Curri, "Multi-Vendor Experimental Validation of an Open Source QoT Estimator for Optical Networks," *J. of Lightwave Tech.*, vol. 36, pp. 3073–3082, aug 2018.
- [5] V. Curri, P. Poggiolini, A. Carena, and F. Forghieri, "Dispersion compensation and mitigation of nonlinear effects in 111-gb/s wdm coherent pm-qpsk systems," *IEEE Photonics Technology Letters*, vol. 20, no. 17, pp. 1473–1475, 2008.
- [6] A. Carena, V. Curri, P. Poggiolini, and F. Forghieri, "Guard-band for 111 gbit/s coherent pm-qpsk channels on legacy fiber links carrying 10 gbit/s imdd channels," in *OFC 2009*, pp. 1–3, 2009.
- [7] J. Renaudier, O. Bertran-Pardo, G. Charlet, M. Salsi, M. Bertolini, P. Tran, H. Mardoyan, and S. Bigo, "Investigation on wdm nonlinear impairments arising from the insertion of 100-gb/s coherent pdm-qpsk over legacy optical networks," *IEEE Photonics Technology Letters*, vol. 21, no. 24, pp. 1816–1818, 2009.
- [8] A. Carena, G. Bosco, V. Curri, Y. Jiang, P. Poggiolini, and F. Forghieri, "Egn model of non-linear fiber propagation," *Optics express*, vol. 22, no. 13, pp. 16335–16362, 2014.
- [9] V. Curri, A. Carena, P. Poggiolini, G. Bosco, and F. Forghieri, "Extension and validation of the gn model for non-linear interference to uncompensated links using raman amplification," *Optics express*, vol. 21, no. 3, pp. 3308–3317, 2013.
- [10] V. Curri, A. Carena, A. Arduino, G. Bosco, P. Poggiolini, A. Nespola, and F. Forghieri, "Design strategies and merit of system parameters for uniform uncompensated links supporting nyquist-WDM transmission," *J. of Lightwave Tech.*, vol. 33, pp. 3921–3932, sep 2015.
- [11] P. Poggiolini et al., "The GN-model of fiber non-linear propagation and its applications," *IEEE / OSA JLT*, vol. 32.4, pp. 694–721, 2014.
- [12] P. Johannisson and M. Karlsson, "Perturbation analysis of nonlinear propagation in a strongly dispersive optical communication system," *J. of Lightwave Tech.*, vol. 31, no. 8, pp. 1273–1282, 2013.
- [13] R. Dar, M. Feder, A. Mecozzi, and M. Shtaif, "Pulse collision picture of inter-channel nonlinear interference in fiber-optic communications," *Journal of Lightwave Technology*, vol. 34, no. 2, pp. 593–607, 2016.
- [14] E. Virgillito, A. Castoldi, A. D'Amico, S. Straullu, S. Abrate, R. Pastorelli, and V. Curri, "Propagation effects in mixed 10g-100g dispersion managed optical links," in *ICTON 2019*, p. We.D1.5, 2019.
- [15] D. Marcuse, C. R. Manyuk, and P. K. A. Wai, "Application of the manakov-pmd equation to studies of signal propagation in optical fibers with randomly varying birefringence," *Journal of Lightwave Technology*, vol. 15, no. 9, pp. 1735–1746, 1997.
- [16] E. Virgillito, S. Straullu, A. Castoldi, R. Pastorelli, and V. Curri, "Non-linear snr degradation of mixed 10g/100g transmission over dispersion-managed networks," in *ICTON*, p. We.C2.5, 2020.
- [17] A. Viterbi, "Nonlinear estimation of psk-modulated carrier phase with application to burst digital transmission," *IEEE Transactions on Information Theory*, vol. 29, no. 4, pp. 543–551, 1983.